Supplementary Information

Size-dependent AuNPs Plasmonic Activity for the Rational Design of Organic Reactions Catalyst

Daria Votkina,[a] Andrii Trelin,[b] Viktor Semin,[c] Oleksiy Lyutakov,[b] Vaclav Svorcik,[b] Pavel Petunin,[a] Gerard Audran,[d] Sylvain Marque,[d] Olga Guselnikova,*[a,e] Pavel Postnikov,*[a,b]

[a] Research School of Chemistry and Applied Biomedical Sciences, Tomsk Polytechnic University, Lenina Avn. 30, Tomsk 634050, Russian Federation.

[b] Department of Solid-State Engineering, University of Chemistry and Technology, Technicka 5, Prague 166 28, Czech Republic

[c] Institute of Strength Physics and Materials Science of Siberian Branch of Russian Academy of Sciences, pr. Akademicheskii 2/4, Tomsk, 634055, Russian Federation

[d]Aix-Marseille University, CNRS, UMR 7273, ICR case 551, Avenue Escadrille Normandie-Niemen, Marseille 13397 Cedex 20, France

[e] Centre of electrochemical and surface technology, Viktor Kaplan Straße 2, 2700 Wiener Neustadt, Austria.

Table of Content

Section S1. Transmission electron microscopy images for size AuNPs investigation 2
Section S2. Calculation of AuNPs optical properties 3
Section S3. Kinetic investigations 4
Section S4. Quantum Yield calculation 8
Section S5. Long-term stability study 9

Section S1. Transmission electron microscopy images for size AuNPs investigation

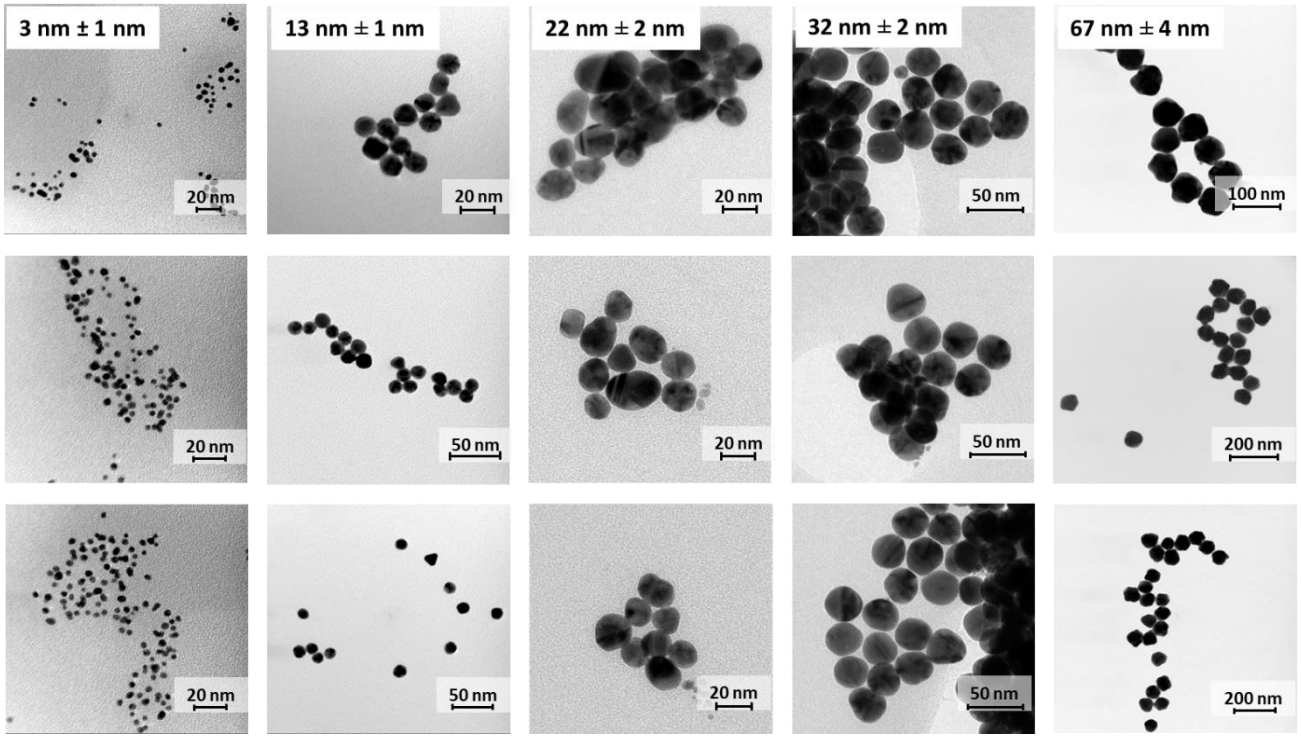

Figure S1. TEM images of gold nanoparticles with 3, 13, 22, 32 and 67 nm diameter.

Section S2. Calculation of AuNPs optical properties

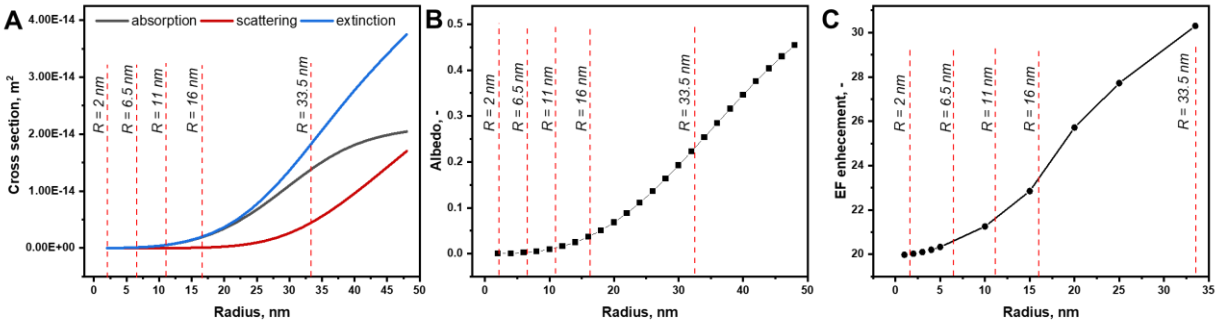

Figure S2. Calculated according to Mie theory A) Absorption, scattering and extinction cross sections. B) Albedo. C) EF enhancement

Table S1. The main parameters studied AuNPs

	AuNPs size, nm				
	3 ± 1	13 ± 1	22 ± 2	32 ± 2	67 ± 4
[Au] mg/L of stock solution	9.75	40.8	34.5	52	33
Volume of stock solution that was taken for reaction, µL	2400	573	678	450	710
Surface area, m^2/L[a]	0.781	0.180	0.110	0.075	0.036
EF enhancement[b], -	20.04	20.6	21.90	22.86	30.03
Absorption cross section[b], m^2	2.9E-18	8.0E-17	4.2E-16	1.6E-15	1.2E-14
Scattering cross section[b], m^2	2.2E-22	1.6E-19	3.6E-18	6.3E-17	3.6E-15

[a] Surface area of NP was calculated by assuming same size for all NPs. With this assumption, surface area per unit volume is given by $S = \frac{3C}{\rho r}$, where C is gold concentration, ρ - gold density, r - NP radius. [b] EF enhancement, absorption and scattering cross-sections, albedo was calculated from Mie theory.

Section S3. Kinetic investigations

4-nitrophenol reduction without light irradiation

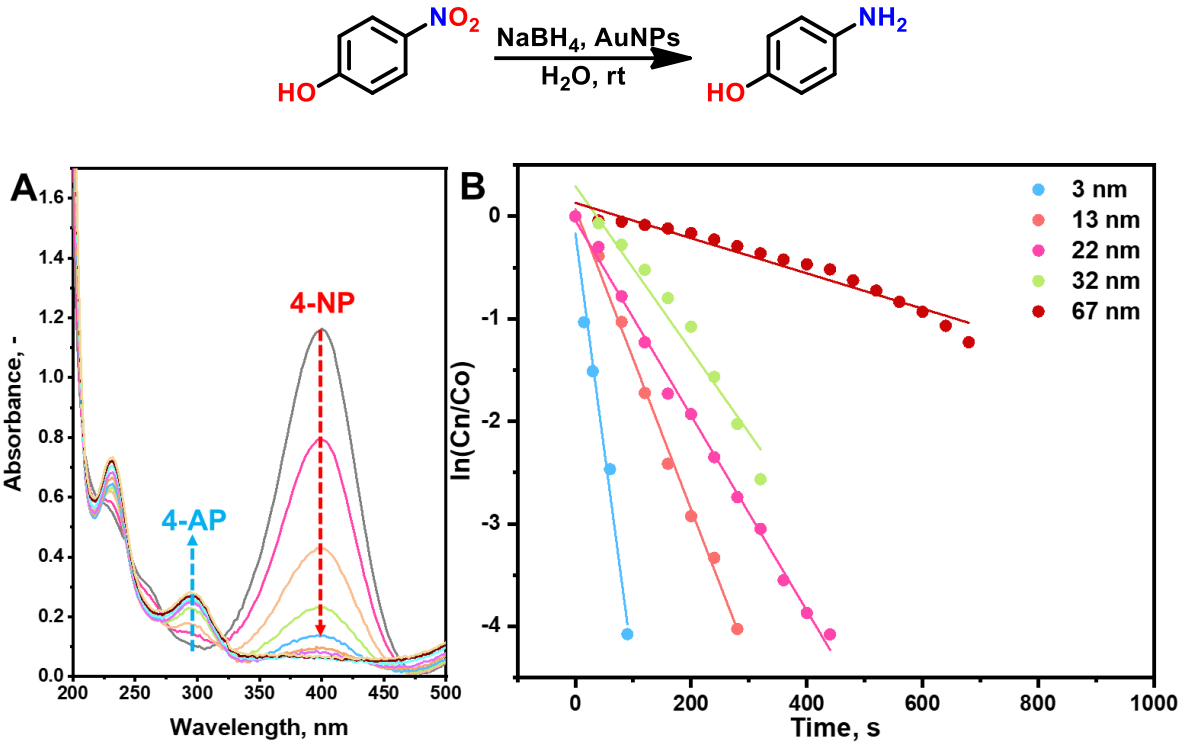

Figure S3. A) Kinetic investigation of 4-NP reduction to 4-AP monitored by UV-Vis. B) Linearized kinetic curves of 4-NP reduction in presence of $NaBH_4$ and AuNPs with different size.

Plasmon-driven 4-nitrophenol reduction

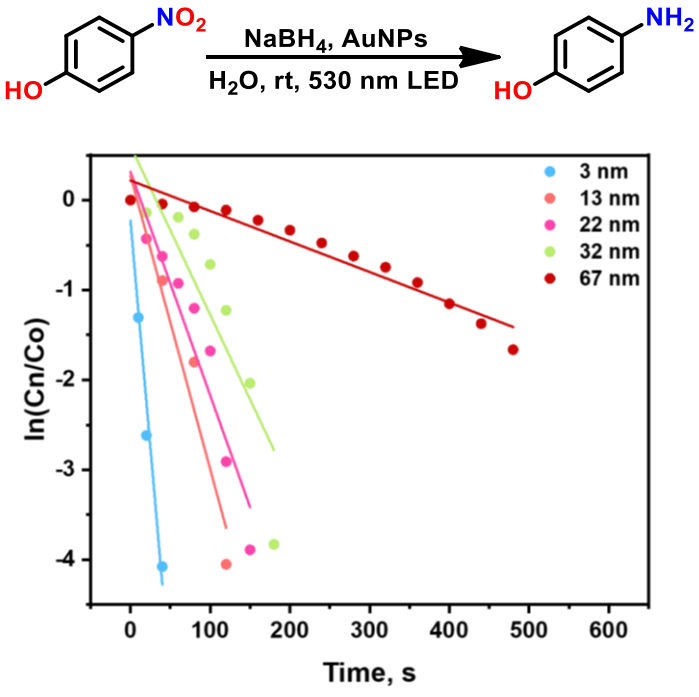

Figure S4. Linearized kinetic curves of 4-NP reduction in presence of $NaBH_4$ and AuNPs with different size under 530 nm LED irradiation. using equation.

Table S2. Rate constants of 4-NP reduction without irradiation and under plasmon-irradiation.

AuNPs	In the dark			Plasmon-assisted			$\frac{k_{plasmon}}{k_{dark}}$
	k^a, $(10^2\ s^{-1})$	R^2	TOF, $(10^2\ s^{-1})$	k^a, $(10^2\ s^{-1})$	R^2	TOF, $(10^2\ s^{-1})$	
3 nm	4.2	0.98	2.80	8.7	0.99	6.30	2.07
13 nm	1.40	0.99	0.90	3.2	0.91	2.10	2.28
22 nm	0.95	0.98	0.70	2.5	0.92	1.68	2.63
32 nm	0.80	0.95	0.30	1.1	0.75	1.40	1.375
67 nm	0.27	0.74	0.28	0.5	0.86	0.4	1.85

[a]Rate constant was calculated according to $\ln\left(\frac{C_n}{C_0}\right) = -k * t$, where Cn – concentration of 4-NP at a certain point in time (M). C_0 – initial concentration of 4-NP (M), k – rate constant, (s^{-1}).

BBY degradation

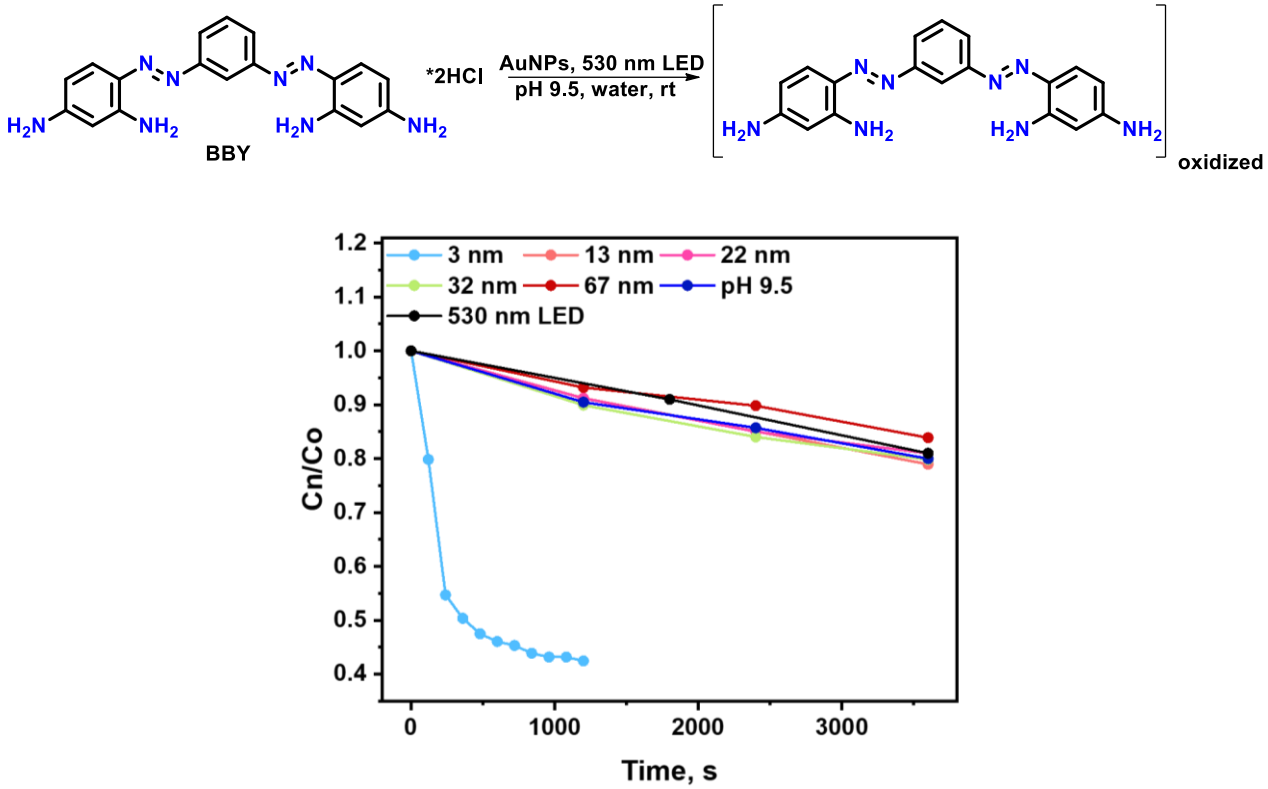

Figure S5. Control experiments for BBY degradation. *Dark blue line* – decrease of BBY concentration in alkali media. *Black line* – degradation without AuNPs under 530 nm LED irradiation. *Blue line* – degradation in presence of 3 nm AuNPs in the dark. *Pink line* – degradation in presence of 13 nm AuNPs in the dark. *Magenta line* – degradation in presence of 22 nm AuNPs in the dark. *Green line* – degradation in presence of 32 nm AuNPs in the dark. *Red line* – degradation in presence of 67 nm AuNPs in the dark.

Table S3. Calculation of degradation efficacy of BBY at 1800 s

AuNPs	Degradation efficacy at 1800 s,[a] %		TOF, (10^3 s^{-1})
	in the dark	plasmon-driven	
3 nm	59	73	2.05
13 nm	12	68	1.91
22 nm	13	55	1.60
30 nm	13	42	1.18
60 nm	9	32	0.90

[a] The degradation efficiencies were calculated according to % = $\left(1-\frac{Cn}{Co}\right) * 100$ at 1800 s.

C-ON bond homolysis of alkoxyamine

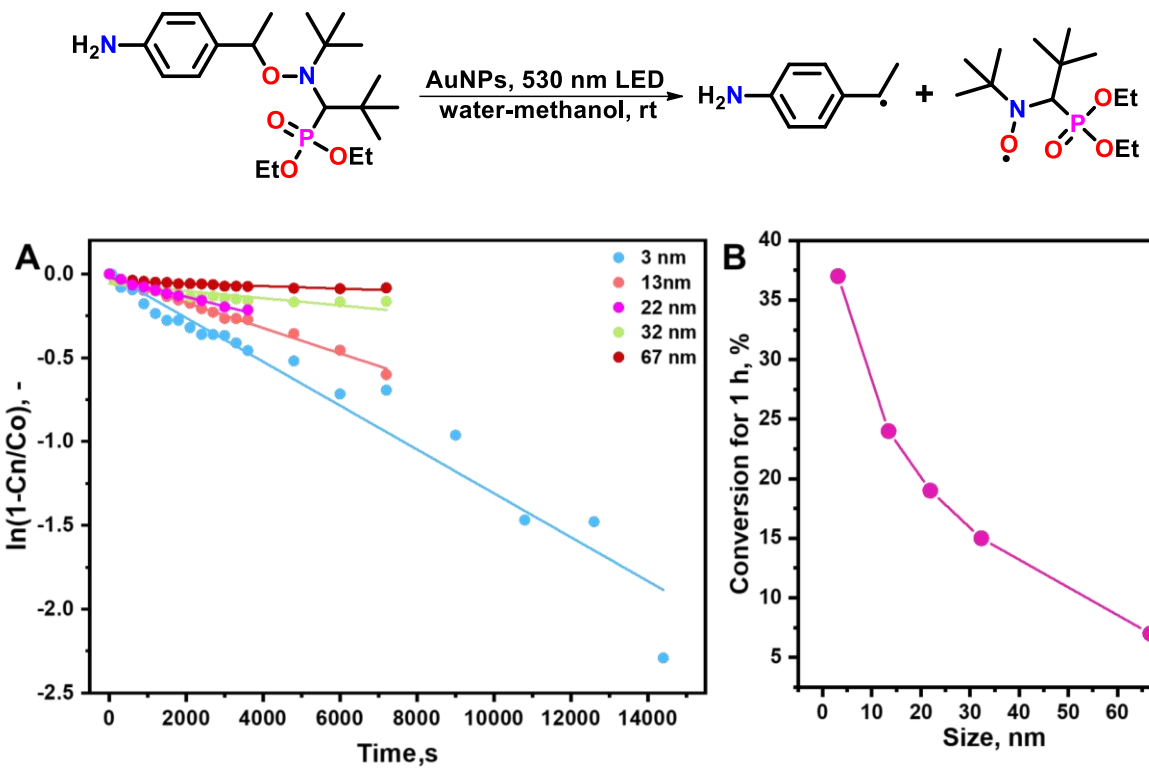

Figure S6. A) Linearized kinetic curves of plasmon-induced alkoxyamine homolysis. B) Conversion of alkoxyamine for 1 hour in plasmon-driven homolysis.

Table S4. Rate constants of plasmon-induced homolysis of alkoxyamine **SG1-St-NH₂** at room temperature in water.

AuNPs	Rate constant,[a] (10^4 s^{-1})	R^2	TOF, (10^4 s^{-1})
3 nm	1.2	0.96	2.07
13 nm	0.96	0.98	1.58
22 nm	0.67	0.95	1.46
32 nm	0.29	0.73	0.84
67 nm	0.14	0.81	0.42

[a] Rate constant was calculated according to $\ln\left(\frac{C_n}{C_0}\right) = -k * t$, where Cn – concentration of 4-NP at a certain point in time (M). C_0 – initial concentration of 4-NP (M), k – rate constant, (s^{-1}).

Section S4. Quantum Yield calculation

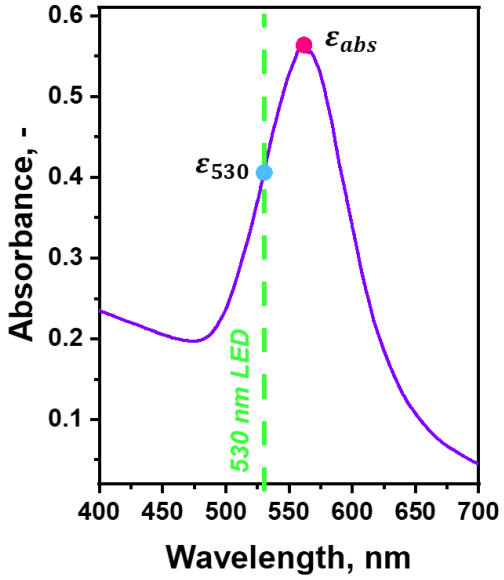

Figure S7. The estimation of absorbed light amount by nanoparticles using UV-Vis of AuNPs in water.

Table S5. Calculation of quantum yields of studied reactions

	Quantum yield, %				
	3 nm	**13 nm**	**22 nm**	**32 nm**	**67 nm**
4-NP reduction	8.91	3.38	2.59	1.11	0.3
BBY oxidation	4.25	3.92	3.09	2.35	1.04
Alkoxyamine homolysis	4.3E-3	3.4E-3	2.3E-3	9.8E-4	2.85E-4

Section S5. Long-term stability study

Catalytic cycle repetition

In three vessels (marked as I, II, and III), the appropriate volume of different-size AuNPs solutions (volumes of stock solutions are provided in Table S1) was mixed with an alkoxyamine SG1-St-NH_2 solution in methanol (0.1 mM, 0.3 mL). Finally, the Milli-Q water has been added to maintain the volume equal to 3 mL in each vessel. The reaction mixture in all vessels was stirred and irradiated at the same time with LED (530 nm, 63 mW cm^{-2}) located directly above the reaction mixture (20 mm) at room temperature. The first catalytic cycle was carried out in vessel I by the sampling in appropriate time and analyzing by EPR at 25 °C. After full conversion of alkoxyamine in vessel I, the fresh portion of alkoxyamine was added to the vessel II and the kinetic measurements of the second catalytic cycle were started by the sampling from vessel II in appropriate time with further analyzing by EPR. After full conversion of alkoxyamine in the vessel II, the third cycle started with adding new portion of SG1-St-NH_2 to the vessel III. The kinetic measurement procedure was repeated as previously described.

Table S6. Rate constants and turnover frequency values over three cycles of plasmon-driven homolysis.

Size of AuNPs, nm	Catalytic cycle	k_d, (10^4 s^{-1})	R^2	TOF, (10^4 s^{-1})
3	I	1.21	0.96	2.07
	II	0.51	0.99	0.98
	III	0.39	0.98	0.88
13	I	0.96	0.98	1.58
	II	0.32	0.96	0.55
	III	0.13	0.98	0.24
67	I	0.14	0.81	0.42
	II	No full conversion on the I cycle		
	III			

Related discussion to Table S6 and Fig. 6C (main text)

According to Table S6, after the second cycle of AA homolysis using 3 nm AuNPs, the efficacy was reduced to 47 % cycle and to 42% for the third one, whereas for 13 nm AuNPs utilization TOF_{conc}. dropped dramatically to 35 % and 15 % for the second and third cycles, respectively. The larger 67 nm nanoparticles did not allow the full conversion and made it impossible to repeat several catalytic cycles.

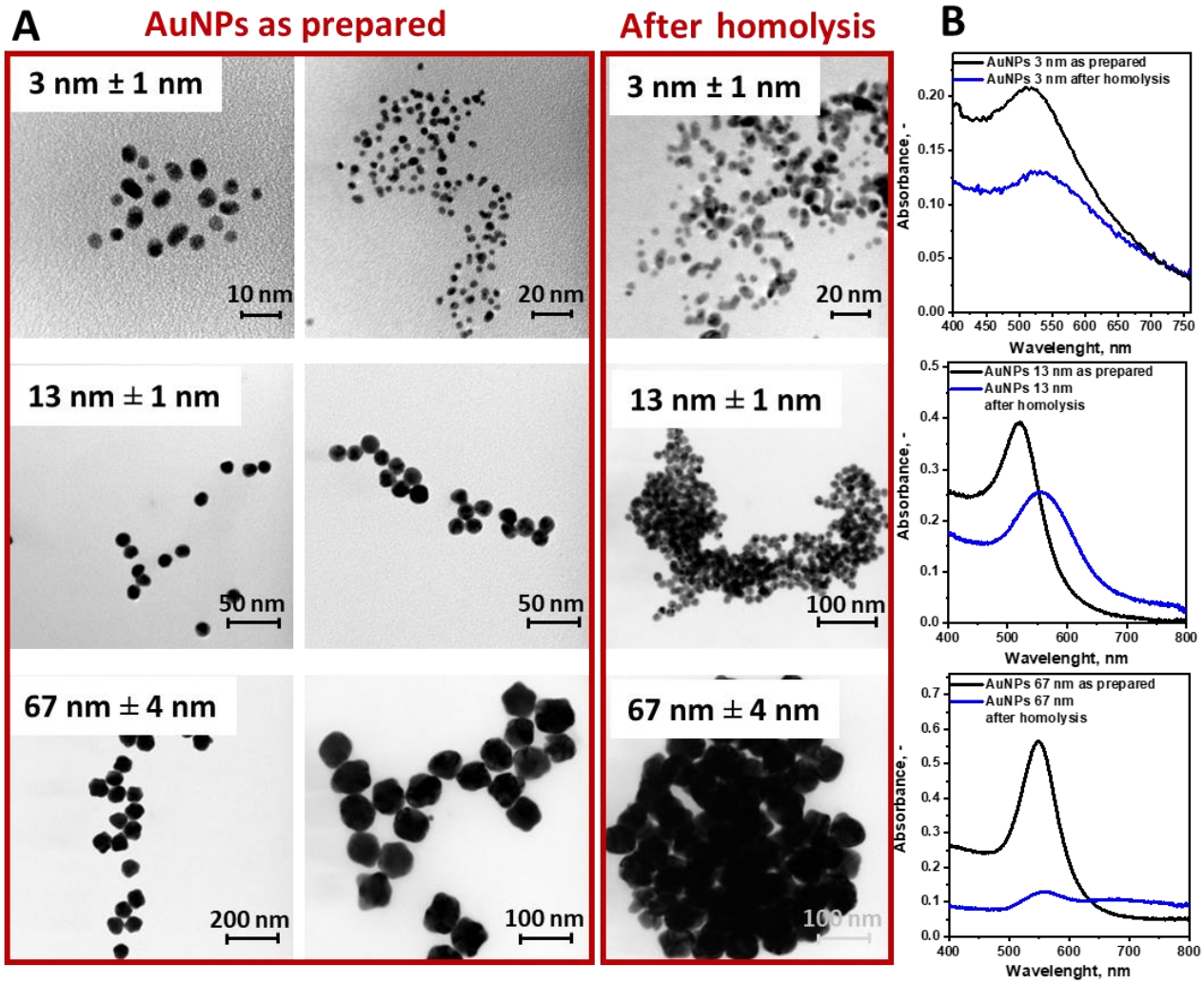

Figure S8. AuNPs stability in plasmon-induced homolysis of alkoxyamine. A) TEM images of 3, 13 and 67 nm AuNPs as prepared and after homolysis. B) UV-Vis spectra of 3, 13 and 67 nm AuNPs before and after homolysis.

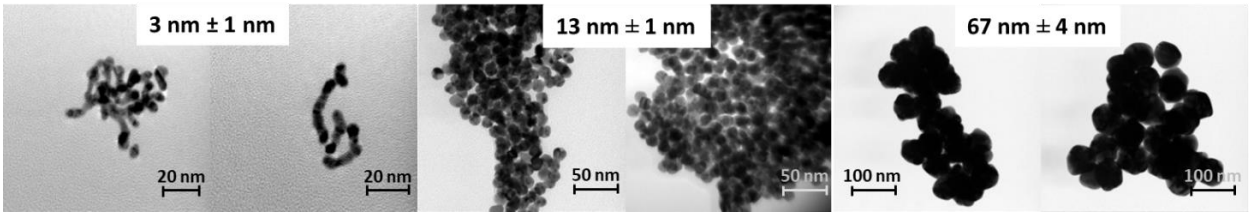

Figure S9. TEM images of 3, 13, 67 nm AuNPs after plasmon-induced 4-NP reduction.